Journal of Computers Vol. 27, No. 4, 2016, pp. 1-14
doi:10.3966/199115592016122704001

The Fault Feature Extraction of State Signal in Control Systems Based on Joint Noise Reduction Method and Empirical Mode Decomposition

Pu Yang[1*], Rui-Cheng Guo[1], Xu Pan[1], and Jian-Wei Liu[1]

[1] College of Automation Engineering, Nanjing University of Aeronautics and Astronautics, Nanjing 210016, Jiangsu, China
ppyang@nuaa.edu.cn

Received 5 May 2015; Revised 11 August 2015; Accepted 28 August 2015

Abstract. In this paper, the joint noise reduction method and empirical mode decomposition (EMD) are proposed to solve the problem about fault feature extraction of state signals in control systems. In order to restrain impulse noises and Gauss white noises effectively, the improved wavelet threshold noise reduction method combined with median filter is given. The method of endpoint extension, ensemble empirical mode decomposition (EEMD) and correlation coefficient threshold comparison are proposed to overcome the endpoint effect, mode mixing and pseudo components of EMD and to improve the accuracy and rapidity of fault feature extraction. Results of numerical simulation and quad-rotor semi-physical simulation platform test verify the effectiveness and feasibility of the method mentioned in this paper.

Keywords: EMD, fault real-time detection, feature extraction, wavelet threshold noise reduction

1 Introduction

1.1 Research background

Since the composition of modern control system, which often works under different environmental conditions in high load for a long time, is more and more complex and it will cause kinds of faults inevitably. Especially in the aerospace, medical, large-scale machinery production and other fields, subtle faults may cause serious economic loss and personnel injury. So the running condition monitoring and fault detection of equipment are becoming an important research topic. The prerequisite of accurate condition monitoring and fault detection is to obtain feature information of the running state of control systems. The state signal of control systems is a typical non-stationary signal, and especially the fault signal occurred in fault control systems. At the same time, the difficulty of signal identification and fault feature extraction increases because of the anisotropy of transmission media and noise influence.

1.2 Related works

Empirical mode decomposition (EMD) proposed by Huang [1-2] is an analysis method that is suitable for nonlinear and non-stationary signal. The signal is decomposed into a series of different frequency components of intrinsic mode function (IMF) through EMD, which makes the instantaneous frequency of the signal has practical significance, instead of sine/cosine function through Fourier transform. Compared with other signal processing methods, EMD is more intuitive, direct and adaptive. Zhu et al. [3] decomposes signals by ICA-EMD. Independent component analysis (ICA) is not affected by strong noise and interference but the mixing model and unmixing model of ICA are similar to the neural network and the inappropriate parameter selection may cause the divergence. Cui et al. [4] uses the EMD combined with

* Corresponding Author

the correlation coefficient to extract signal features, which eliminates pseudo IMF components to a certain extent, but the end effect and mode mixing inherent in EMD are ignored so that it causes some error. In order to eliminate the end effect, Qiu et al. [5] uses the Volterra model to predict the endpoint data and to do the endpoint extension, but the prediction accuracy decreases with the passage of time. Yang et al. [6] eliminates the end effect by using the prediction method based on the maximum Lyapunov exponent. It is not easy to determine a linear region in the process of calculating the largest Lyapunov exponent, although this method is useful for the endpoint extension in nonlinear system. Yang et al. [7] solves the end effect via a new end extending algorithm in which a new computation parameter is applied to estimate the similarity between two waveforms. However, the parameters designed are so arbitrary that the efficiency of this algorithm is restricted. The improvement of EMD at low sampling frequency is given in paper [8], where oil pipeline leakage faults achieve the expected results well. However, the sampling frequency of actual control system state signal is often very high, so this method cannot be applied to the feature extraction of state signals in control systems. The IMFs contained signal features are selected by EMD in paper [9-12], although this method is feasible for high signal-to-noise ratio, the accurate IMFs will not be able to be decomposed for the signal contained too many noises and interferences. Because the signal collected from control system often includes strong random noises, the noise reduction processing must be first on the sampling signal before extracting feature.

Wavelet transform is a time-space frequency localization analysis [13-14]. The noise reduction method based on wavelet transform can indicate local information of signals in the time and frequency domain effectively and has the multi-resolution characteristic. Paper [15] studies the effect of signal noise reduction via wavelet transform which shows a great advantage of denoising especially restraining nonlinear random noises compared with the effect of signal noise reduction via Fourier transform. The main methods at present are modulus maximum value algorithm, spatial correlation algorithm and wavelet threshold algorithm which is most widely used. New thresholds and new threshold functions are selected to improve the wavelet threshold algorithm [16-21], and noises of signals are restrained to varying degrees. However, the number of decomposition layers is selected by experience, and Gauss white noises are able to be restrained effectively while the influence of impulse noises is not to be considered at the same time.

Besides, the end effects and the mode mixing are two main problems to restrict the development of EMD. The main reason of the end effect is the fitting error caused by the spline interpolations, which will cause the further error influences with the decomposition process, due to the initial signal endpoint is not the extreme point. The mode mixing is a phenomenon that one mode includes different other modes because the mode components are unable to effectively isolated from each other.

Based on the above analysis, this paper proposes a fault feature extraction method of state signal in control systems through the joint noise reduction method and EMD decomposition. Firstly, the abnormal values of signal amplitude caused by impulse noises are removed by the median filter. Then the improved wavelet threshold noise reduction is used to restrain Gauss white noises. In the improved wavelet threshold noise reduction, the selection of threshold and threshold function, processing of the wavelet coefficients near thresholds and determination of the number of decomposition layers are illustrated. Simultaneously, the signal after the noise reduction is decomposed by the improved EMD and the energy entropy indicated characteristics of the signal is established. The improved EMD not only eliminates the end effect and mode mixing effectively, but also removes some pseudo components by the correlation coefficient threshold comparison method to reduce some calculations and increase real time significantly. Finally, the feasibility and effectiveness of the method proposed in this paper are verified by the numerical simulation and the experiment of Qball-X4 quad-rotor helicopter semi-physical simulation platform.

2 Joint Noise Reduction Method

2.1 Preliminaries of control system

A complete closed-loop control system mainly includes controllers, sensors, actuators and controlled objects. In the actual operation, the fault of any part of a system will be reflected in a state signal, so the state signal of a system must be collected to extract the fault feature information in order to monitor the health status of control system in real-time.

Suppose the sampling discrete signal with noises as formula (1).

$$f(k)=s(k)+n(k)=s(k)+r(k)+z(k) \quad (k=1,2,...,N) \tag{1}$$

Among them, $f(k)$ is the signal with noises, $s(k)$ is the effective signal without noises, $n(k)$ is the noise, $r(k)$ is the Gauss white noise, $z(k)$ is the impulse noise and N is the length of sampling signal.

2.2 The median filter noise reduction

Take the signal with noises $f(k)(k=1,2,...,N)$ to median filter and the signal $\tilde{f}(k)$ filtered out impulse noises $z(k)$ can be obtained.

Let $f(k)(k=1,2,...,N)$ extract medians in accordance with the center k and length n. Then $\tilde{f}(k)$ is shown as formula (2).

$$\tilde{f}(k)=med(f(k))=\begin{cases} f\left(\dfrac{(n+1)}{2}\right), & n \text{ is the odd number} \\ \dfrac{1}{2}\left(f\left(\dfrac{n}{2}\right)+f\left(\dfrac{(n+2)}{2}\right)\right), & n \text{ is the even number} \end{cases} \tag{2}$$

2.3 The improved wavelet threshold noise reduction

Take $\tilde{f}(k)$ to do wavelet threshold noise reduction and filter out the Gauss white noise $r(k)$ and then obtain the estimated signal without noises $\hat{s}(k)$.

2.3.1 The determination of the number of the decomposition layers

In the actual process, because of different signals and different signal-to-noise ratios, the optimal number of decomposition layers is inevitably different to achieve the best noise reduction [22]. This paper uses the following method to determine the number of decomposition layers. Firstly, take $\tilde{f}(k)$ to do the No. j layer wavelet decomposition ($j=1,2,...$), and to obtain the approximate coefficient of low frequency $a_j(k)$ and the approximate coefficient of high frequency $d_j(k)$. Secondly, calculate autocorrelation coefficient $\lambda_{j,i}$ according to formula (3).

$$\lambda_{j,i}=\frac{\sum_{k=0}^{N-i}\left[d_j(k)-\bar{d}_j\right]\left[d_j(k+i)-\bar{d}_j\right]}{\sum_{k=0}^{N-i}\left[d_j(k)-\bar{d}_j\right]^2}, i=1,2,...,l \tag{3}$$

Among them, $d_j(k)$ is the approximate coefficient of high frequency, $\bar{d}_j$ is the average of $d_j(k)$ and l generally takes $\left\lceil N/2 \right\rceil$.

Finally, if $\lambda_{j,1}^2+\lambda_{j,2}^2+...+\lambda_{j,l}^2 \sim \chi^2(l)$, to take the No. $j+1$ layer wavelet decomposition. Unless the approximate coefficient of high frequency $d_{\Delta+1}(k)$ does not meet $\lambda_{\Delta+1,1}^2+\lambda_{\Delta+1,2}^2+...+\lambda_{\Delta+1,l}^2 \sim \chi^2(l)$, the number of decomposition layers is Δ and remaining all wavelet coefficients W_j.

2.3.2 The choice of threshold and threshold function

The appropriate choice of threshold and threshold function is the prerequisite in which removing noises of the signal to the greatest extent.

In the process of the threshold determination, if the threshold is too small, then a lot of noises are still remained; if the threshold is too large, the effective signal may be filtered as noises. This paper puts forward the threshold taken into account the fact that the wavelet coefficients of noises decrease along with the increase of the scale.

$$\delta = \frac{\sigma\sqrt{2\ln(N)}}{\sqrt{j}} \tag{4}$$

Among them, σ is the standard deviation of noises and $j\left(j=1,2,...,\Delta\right)$ is the decomposition scale.

Not only the threshold considers the relation between the standard deviation of noises and the length of sampling signal, but also the effect of decomposition scales is added into this threshold, which improves noise reduction rate and keeps the effective signal.

The continuity and accuracy of signal reconstruction are affected greatly by the choice of threshold function. In order to avoid additional oscillation caused by function discontinuity and eliminate a constant deviation between the wavelet coefficient before and after processing by the threshold function, this paper presents an improved threshold function as formula (5).

$$W_{\delta j} = \begin{cases} \text{signal}\left(W_j\right)\left(\left|W_j\right| - \dfrac{2p}{1+e^{q\left(\left|W_j\right|-\delta\right)}}\delta\right), \left|W_j\right| \geq \delta \\ W_j \cdot \varphi^{-\left(\mu\left|W_j\right|-\delta\right)^2}, \left|W_j\right| < \delta \end{cases} \tag{5}$$

Among them, W_j is the wavelet coefficient of $\tilde{f}\left(k\right)$, δ is the threshold, $W_{\delta j}$ is the wavelet coefficient after noise reduction. $\mu\left(\mu>0\right)$, $p\left(0\leq p\leq 1\right)$, $q\left(q\geq 0\right)$ are all adjustable parameters and φ is a constant more than 1.

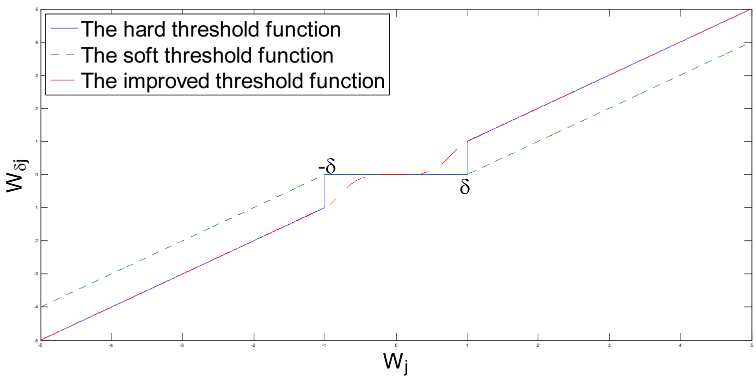

Fig. 1. The comparison of different threshold functions

Fig. 1 shows the comparison of different threshold functions. It can be concluded that this improved threshold function not only has the continuity of the soft threshold function when it can overcome the constant deviation, but also avoids the disadvantages of the hard threshold function and preserves the edge details of the signal.

For the selection of adjustable parameters p, q, μ, it can be concluded that: when $p=0$, q takes any value, this threshold function is approximated as the hard threshold function; when $0<p\leq 1$ and $q=0$, this threshold function is approximated as the soft threshold function; when $p=0, \varphi>1$, if μ is larger, then this threshold function is closer to the hard threshold function. It can be concluded that the changes of the value of p can adjust the compressibility for wavelet coefficient of this threshold function to make up for the lack of soft threshold functions. The changes of the value of q, μ mainly determine the tendency of this threshold function.

2.3.3 The inter-scale correlation of the wavelet transform

In the wavelet threshold noise reduction process, it is a problem worthy of attention that ways to improve the accuracy of judgment of the wavelet coefficients near thresholds, in order to improve the noise reduction effect. The inter-scale correlation of the wavelet transform is a common method [23]. In order to avoid a large number of computations effectively, this paper uses the following method to deal with the wavelet coefficients near thresholds. Firstly, the inter-scale correlation amount θ of wavelet coefficients W_j which is in $\left[\delta(1-\alpha),\delta(1+\alpha)\right]$ ($0<\alpha\le 0.1$ is adjustable factor) is calculated by formula (6).

$$\theta=\ln\left(\frac{\max W_j}{\min W_j}\right) \tag{6}$$

Among them, W_j is the wavelet coefficient of $\tilde{f}(k)$ at layer $j\left(j=1,2,...,\Delta\right)$, $\max W_j$ and $\min W_j$ are respectively the maximum and the minimum of $\left|W_j\right|$ ($j=1,2,...,\Delta$).

Secondly, mark all wavelet coefficients W_j belonging to $\theta\in\left[0,\beta\right]$ ($\beta>0$ is adjustable factor)as W_j^1 and the rest as W_j^2. Thirdly, the wavelet coefficients are dealt with by formula (5), where W_j^1 is considered as the condition $\left|W_j\right|\ge\delta$ and W_j^2 is considered as the condition $\left|W_j\right|<\delta$. Finally, take the wavelet coefficients $W_{\delta j}$ to do the inverse wavelet transformation and obtain the estimation of the signal without noises $\hat{s}(k)$.

From the above discussion, the inter-scale correlation can be determined to improve the effect of noise reduction. If the value of β is too small, then $\max W_j$ is too close to $\min W_j$, the estimation of inter-scale is too harsh, so the useful information of signals may be filtered. If the value of β is too large, the wavelet coefficient of noises may be remained. Therefore, β should be chosen suitability according to the actual requirement of noise reduction. Generally, β is less than 10.

3 The Design of Feature Extraction Method Based on EMD

3.1 The method to restrain the end effect

In order to eliminate the end effect, this paper designs a new extension method. The main idea of this method is that a most similar waveform is found in the signal itself, and then use this section of the waveform to do the endpoint extension. The endpoint extension includes the left extension and the right extension. Take the right extension as an example.

Firstly, all the maxima and minima of $\hat{s}(k)$ are respectively marked as $\left\{m_1',m_2',...,m_c'\right\}$ and $\left\{m_1,m_2,...,m_c\right\}$. The waveform section from the right endpoint to m_1 is marked as the signal segment to be extended ω_1 and its length is L. The length from the right endpoint to m_1' is L' (Suppose $L'<L$).

Secondly, let the signal segment be extended ω_1 move from right to left to find the best matching waveform. In the process of the waveform move, take m_1' as the reference point and keep m_1' always coincides with the No. i maximum m_i'. Then calculate the matching coefficient ξ_i of ω_1 and the No. i signal segment to be matched by formula (7). The best matching waveform is the signal segment when ξ_i is smallest.

$$\xi_i=\frac{\sum_{h=1}^{L}\left|\hat{s}\left(m_i'-L+L'+h\right)-\hat{s}\left(m_1'-L+L'+h\right)\right|}{\exp\left(\frac{\operatorname{cov}\left(\hat{s}_{m_i'},\hat{s}_{m_1'}\right)}{\sqrt{D\left[\hat{s}_{m_i'}\right]}\cdot\sqrt{D\left[\hat{s}_{m_1'}\right]}}\right)} \tag{7}$$

Among them, $\mathrm{cov}\left(\hat{s}_{m_i'},\hat{s}_{m_1'}\right)$ the covariance of ω_1 and ω_i and $D[\bullet]$ is the variance.

Finally, extend the best matching waveform to the right of $\hat{s}(k)$ from the left first sampling point of the right endpoint of the best matching waveform and obtain the signal after right extension $\tilde{s}(k)$ (The number of extension point is $INT(N/c)$ generally).

3.2 The solution of mode mixing and pseudo components

For the mode mixing, EEMD is a better way to solve this problem [24-25]. EEMD uses the statistical properties of the noise and the principle of EMD scale separation, making the EEMD can truly become arbitrary data binary filter banks. The principle of EEMD is that a white noise is added to the signal and different scales of signal regions will be mapped to the appropriate scale. When using the all enough mean values, the noise will be offset. The only lasting part is the signal itself. This paper identifies and eliminates pseudo components by the following method based on EEMD.

Firstly, let the signal after endpoint extension $\tilde{s}(k)$ do EEMD and obtain IMF components so that to eliminate the mode mixing phenomenon.

Secondly, calculate the correlation coefficient ρ_i of each IMF and $\tilde{s}(k)$ by formula (8).

$$\rho_i = \frac{\sum_{k=1}^{N} \tilde{s}(k)\cdot imf_i(k)}{\sigma\left[\tilde{s}(k)\right]\cdot\sigma\left[imf_i(k)\right]} \tag{8}$$

Among them, $\sigma[\bullet]$ is the standard deviation and $imf_i(k)$ is the No. i IMF component.

Finally, compare ρ_i with the default threshold $\zeta = b\max(\rho_i)$ ($b\in[0.05,0.3]$)and eliminate IMF components of ρ_i less than ζ after $\max(\rho_i)$.

3.3 The feature extraction method based on EMD energy entropy

In the process of fault feature extraction of state signal in control systems, the signal energy distribution will change along with state change of control systems. Therefore, this paper extracts IMF energy entropy to judge whether the control system is in fault state.

Firstly, calculate the energy of IMF components $imf_i(k)$ after eliminating pseudo components $E_i = \sum_{k=1}^{N} imf_i^2(k) \quad (i=1,2,\ldots,\eta)$. Secondly, calculate IMF energy entropy by formula (9).

$$H = -\sum_{i=1}^{\eta}\frac{E_i}{\sum_{i=1}^{\eta}E_i}\cdot\ln\left(\frac{E_i}{\sum_{i=1}^{\eta}E_i}\right) \tag{9}$$

4 The Numerical Simulation

As shown in formula (10), in order to verify effectiveness of the above algorithm, a nonlinear signal is constructed to implement the numerical simulation.

$$\begin{aligned} f(t) &= s(t)+r(t)+z(t) = \left[1+\sin(50\pi t)\right]\cdot\left[\cos(20\pi t)+0.2\sin(40\pi t)\right] \\ &+\sin(200\pi t)+r(t)+z(t) \end{aligned} \tag{10}$$

This signal is made up of the effective signal $s(t)$, the impulse noise $z(t)$ and the Gauss noise $r(t)$. Fig.

2 is the waveform of $s(t)$ and $f(t)$. The sampling frequency is 1 kHz, and the number of sampling points is 1024. In this simulation, the parameters set $n = 6, \beta = 2, \alpha = 0.05, b = 0.1, l = 512, \ \mu = 4, \varphi = 2, p = 0.9, q = 100$.

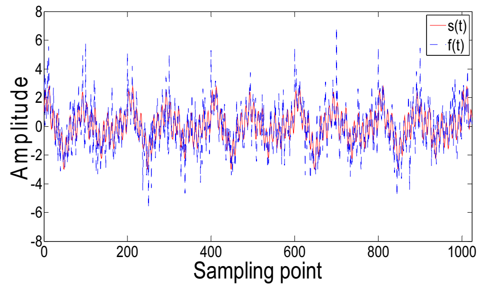

Fig. 2. The waveform of $s(t)$ and $f(t)$

Firstly, take $f(t)$ to median filter as shown in Fig. 3 where impulse noises are restrained well.

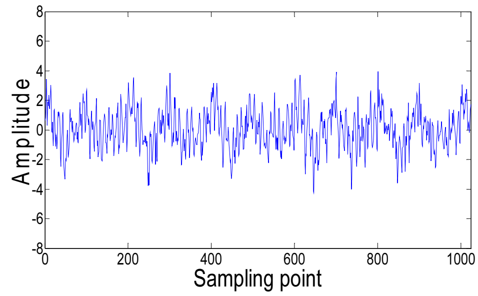

Fig. 3. The waveform after median filter

Secondly, the improved wavelet threshold noise reduction method should be taken. The threshold takes the improved threshold δ mentioned in this paper. Compared with the hard threshold function and the soft threshold function, the result of noise reduction by the improved method proposed in this paper shows in Fig. 4.

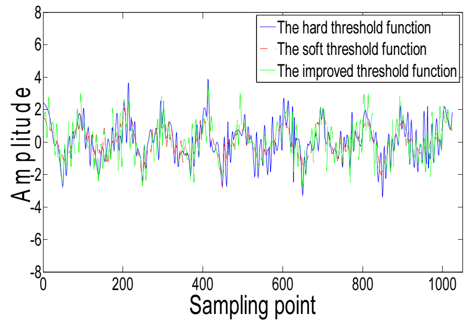

Fig. 4. The waveform of noise reduction by different threshold functions

In order to compare the effect of noise reduction by different methods intuitively, the signal-to-noise *SNR* and mean-square-error *MSE* are introduced. Table 1 shows *SNR* and *MSE* of different methods. Combined with Table 1 and Fig. 2-4, it can be concluded obviously that *SNR* of the improved threshold function is the smallest among three threshold functions and *MSE* of the joint noise reduction method is smaller than the wavelet threshold noise reduction only.

Thirdly, take the signal after the joint noise reduction to do EMD, the obvious endpoint effect and the mode mixing exist from the first IMF as shown in Fig. 5. Therefore, use the improved endpoint extension method to retrain the endpoint effect. Fig. 6 is the pole location, Fig. 7 and Fig. 8 is the matching coefficient of the left extension and the matching coefficient of the right extension at different the order num-

Table 1. The comparison of *SNR* and *MSE* of different noise reduction method

The noise reduction method	*SNR*	*MSE*
The wavelet threshold noise reduction by the hard threshold function	3.4678	1.0578
The wavelet threshold noise reduction by the soft threshold function	2.4469	1.3381
The wavelet threshold noise reduction by the improved threshold function	4.1411	0.9059
The joint noise reduction by the hard threshold function	5.4368	0.5114
The joint noise reduction by the soft threshold function	3.6170	0.7776
The joint noise reduction by the improved threshold function	6.9831	0.3582

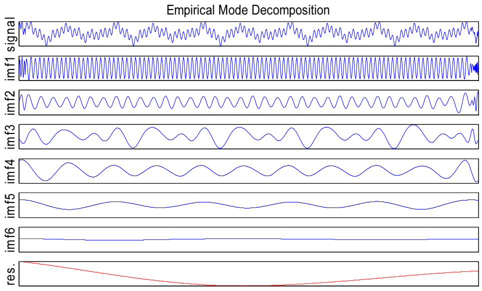

Fig. 5. The EMD drawing before the endpoint extension

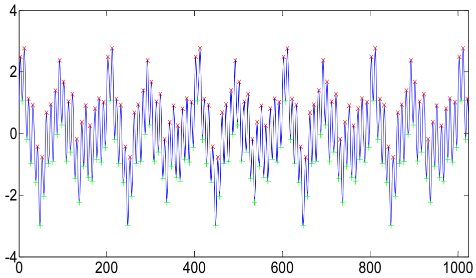

Fig. 6. The pole location

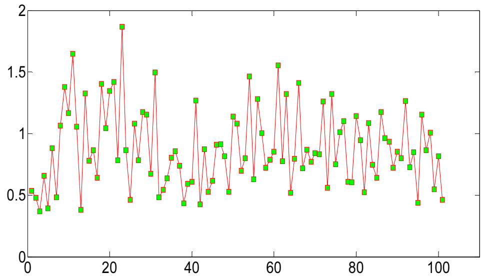

Fig. 7. The matching coefficient of the left extension

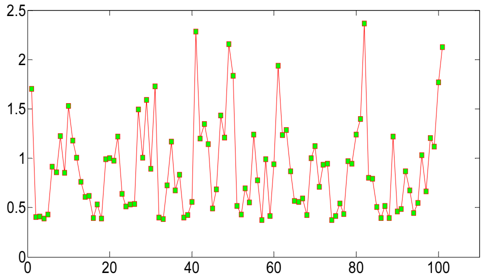

Fig. 8. The matching coefficient of the right extension

ber of extrema. The signal after the endpoint extension is shown in Fig. 9. Then take the signal after the endpoint extension to do EEMD as shown in Fig. 10.

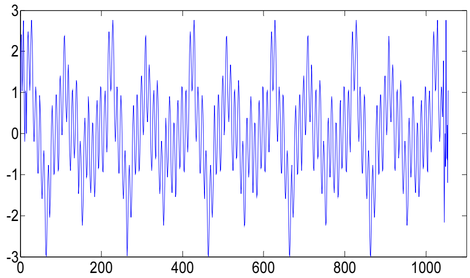

Fig. 9. The signal after the endpoint extension

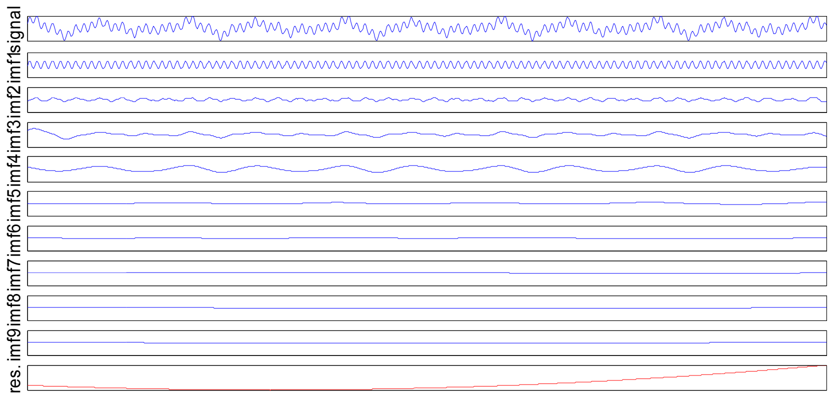

Fig. 10. The EEMD drawing after the endpoint extension

As shown in figure 10, the endpoint effect is restrained well, but the number of IMFs obtained by EEMD is more than EMD, pseudo components may be mixed up in all IMFs. In order to eliminate pseudo components, the correlation coefficient ρ_i is shown in Table 2.

Table 2. The correlation coefficient ρ_i

IMF	1	2	3	4	5
ρ_i	0.6328	0.5114	0.7086	0.6790	0.2191
IMF	6	7	8	9	
ρ_i	0.1046	0.0239	0.0571	0.0552	

Compared with the correlation coefficient ρ_i and the default threshold is $\zeta = 0.1\max(\rho) = 0.07086$, IMF 7, IMF 8 and IMF 9 are all pseudo components because they are all smaller than the default threshold.

Finally, calculate the energy and the energy entropy of each IMF after estimating pseudo components as shown in Table 3.

Table 3. The energy and the energy entropy

IMF	The energy	The energy entropy
1	20.5070	1.6040
2	9.9563	
3	11.8717	
4	15.9226	
5	5.5756	
6	1.5907	

5 The Simulation of Semi-physical Platform

In order to further verify actual application values of the method in control systems, this paper takes the quad-rotor helicopter simulation platform Qball-X4 provided by Quanser Company in Canada as the research object. As shown in Fig. 11, there are six dimension variables (X,Y,Z,ψ,θ,ϕ) in Qball-X4. Among them, X,Y,Z are the location variables, ψ is the yaw angle, θ is the pitch angle, and ϕ is the roll angle. This paper takes the motor speed signal when the quad-rotor helicopter flies in the direction of the X axis as a test object in normal rotor state, minor fault rotor state and severe fault rotor state. The residual signal of the motor speed is collected in real time, and the sampling frequency is 1 kHz, and the number of sampling points is 1000. Fig. 12-14 are respectively the residual signal of the motor speed in normal rotor state, minor fault rotor state and severe fault rotor state.

According to the method mentioned in this paper, the sampling signal should be dealt with by the joint noise reduction method, and then use the improved EMD to decompose the signal after noise reduction. Calculate the energy entropy and determine the running state of control system. In this simulation, the parameters set $n=6, \beta=2, \alpha=0.05, b=0.1, l=512, \mu=4, \varphi=2, p=0.9, q=100$.

The correlation coefficients ρ_i of each IMF of the residual signal of the motor speed after noise reduction in normal rotor state, minor fault rotor state and severe fault rotor state are respectively in Table 4-6. Compared with the default threshold $\zeta_1=0.09428$, $\zeta_2=0.08742$, $\zeta_3=0.09765$, there is no pseudo component in normal rotor state and IMF 6-8 are pseudo components in minor fault rotor state and severe fault rotor state.

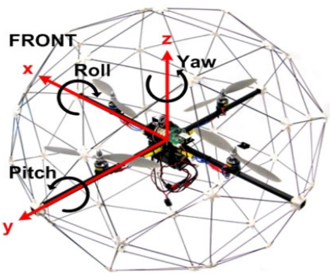

Fig. 11. The body of Qball-X4

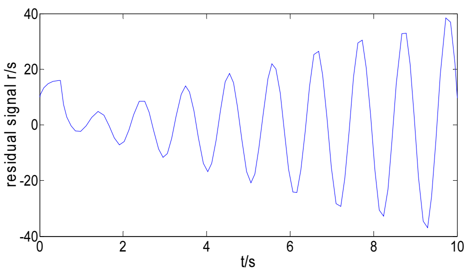

Fig. 12. The residual signal of the motor speed in minor fault rotor state

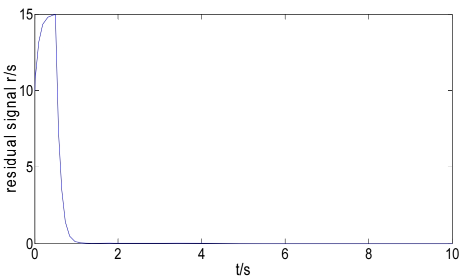

Fig. 13. The residual signal of the motor speed in normal rotor state

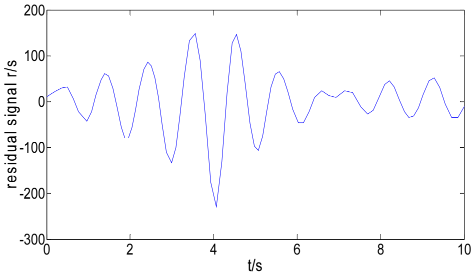

Fig. 14. The residual signal of the motor speed in severe fault rotor state

Table 4. The correlation coefficient of the residual signal of the motor speed after noise reduction in normal rotor state

IMF	1	2	3	4
ρ_i	0.1880	0.3227	0.5291	0.0746
IMF	5	6	7	8
ρ_i	0.1690	0.4168	0.9428	0.7131

Table 5. The correlation coefficient of the residual signal of the motor speed after noise reduction in minor fault rotor state

IMF	1	2	3	4
ρ_i	-0.0036	0.0382	0.8573	0.8742
IMF	5	6	7	8
ρ_i	0.2249	0.0511	0.0032	-0.0215

Table 6. The correlation coefficient of the residual signal of the motor speed after noise reduction in severe fault rotor state

IMF	1	2	3	4
ρ_i	0.0182	0.0011	0.8383	0.9765
IMF	5	6	7	8
ρ_i	0.2198	0.0464	0.0497	0.0290

Table 7-9 are respectively the energy of each IMF after estimating pseudo components and the energy entropy of the state signal of the actuator after noise reduction in normal rotor state, minor fault rotor state and severe fault rotor state. It can be concluded that the energy entropy in normal state is the baggiest, and the energy entropy decreases along with the increase of fault degree.

Table 7. The energy and the energy entropy of the residual signal of the motor speed after noise reduction in normal rotor state

IMF	The energy	The energy entropy
1	0.3261	1.7724
2	0.5049	
3	0.2036	
4	0.4392	
5	0.5358	
6	0.8052	
7	2.5216	
8	1.4027	

Table 8. The energy and the energy entropy of the residual signal of the motor speed after noise reduction in minor fault rotor state

IMF	The energy	The energy entropy
1	0.5460	
2	0.4555	
3	70.1071	0.9289
4	76.4813	
5	10.5412	

Table 9. The energy and the energy entropy of the residual signal of the motor speed after noise reduction in severe fault rotor state

IMF	The energy	The energy entropy
1	3.0336	
2	1.7968	
3	211.3176	0.8524
4	634.1932	
5	88.3941	

Analysis of the results: When the rotor is in normal state, the energy distribution is relatively uniform, so the entropy is larger. When the rotor is in fault state, the energy distribution is in the fault frequency range, so the entropy is smaller. With the increase of fault degree, the energy distribution is more intensive in the fault frequency range. Therefore, the running state of control systems can be determined in real time through the method given in this paper. In addition, the energy entropies are in different sections when faults of actuators, sensors and the controlled objects occur, so this method can also be applied to the fault location in control systems.

6 Conclusion

The state signals in control system often affected by Gauss white noises and impulse noises which will directly affect the feature extraction, and the inaccuracy of the signal feature extraction will cause the misjudgment of the fault detection of control systems. This paper proposes the joint noise reduction method combined with the characteristics of the median filter and the wavelet threshold noise reduction. Especially in the improved wavelet threshold noise reduction, the choice of threshold and threshold function and the processing of the wavelet coefficient belonging to the neighborhood of the threshold both improve the effectiveness of noise reduction. The endpoint extension method and EEMD eliminate the influence of the endpoint effect and the mode mixing. Though the default threshold, pseudo components are filtered out and the calculation is simpler. The numerical simulation and the experiment of Qball-X4 quad-rotor helicopter semi-physical simulation platform both verify the feasibility and effectiveness of the proposed method in this paper.

Acknowledgement

This work is supported by the National Nature Science Foundation of China under Grant No. 61203090 and No. 61374130, the Fundamental Research Funds for the Central Universities under Grant No. NJ20160025 and the Fund of National Engineering and Research Center for Commercial Aircraft Manufacturing under Grant No. SAMC14-JS-15-053.

References

[1] N.E. Huang, Z. Shen, S.R. Long, The empirical mode decomposition and hilbert spectrum for nonlinear and non-stationary time series analysis, Proceedings of the Royal Society 454(1971)(1998) 903-995.

[2] N.E. Huang, Z. Shen, S.R. Long, A new view of nonlinear water waves-hilbert spectrum, Annual Review of Fluid Mechan-

ics 31(1999) 417-457.

[3] W.L. Zhu, J.Z. Zhou, J. Xiao, H. Xiao, C.S. Li, An ICA-EMD Feature Extraction Method and Its Application to Vibration Signals of Hydroelectric Generating Units, Proceedings of the CSEE 33(29)(2013) 95-101.

[4] X.H. Cui, L.Y. Ma, Z.L. Wei, T.H. Wang, Application of wavelet threshold denoising and EMD in instantaneous feature extraction, Machinery and Electronics 32(10)(2014) 12-16.

[5] Y. Qiu, Y.F. Wu, Y.F. Yang, Y. Li, Application of volterra model prediction to end extension of empirical mode decomposition, Journal of Vibration, Measurement and Diagnosis 30(1)(2010) 70-74.

[6] Y.F. Yang, Y.F. Wu, X.M. Ren, W.Y. Qin, X.Z. Zhi, Y. Qiu, The largest lyapunov prediction method for the end issue of empirical mode decomposition, ACTA Physica Sinica 58(6)(2009) 3742-3746.

[7] G. Yang, X.B. Sun, M.X. Zhang, X.L. Li, X.R. Liu, Study on ways to restrain end effect of hilbert-huang transform, Journal of Computer 25(3)(2014) 22-31.

[8] L.Q. Zhao, J.L. Wang, T. Yu, Study on the extraction method for oil pipeline leakage signal feature based on improved empirical mode decomposition, Chinese Journal of Scientific Instrument 34(12)(2013) 2696-2702.

[9] J.Y. Huang, H.W. Yuan, Y. Cui, C.X. Bi, Tire audio signal processing based on EMD and autocorrelation analysis, Journal of Electronic Measurement and Instrumentation 23(9)(2009) 33-37.

[10] S.Q. Zhang, H.L. Shangguan, J.W. Yuan, Y.C. Zhao, J. Yang, Study on the extraction method of characteristic parameters of respiration signals based on intrinsic mode energy ratio, Chinese Journal of Scientific Instrument 31(8)(2010) 1706-1711.

[11] A. Komaty, A.O. Boudraa, J.P. Nolan, D. Dare, On the behavior of EMD and MEMD in presence of symmetric-stable noise, IEEE Signal Processing Letters 22(7)(2015) 818-822.

[12] A. Komaty, A.O. Boudraa, B. Augier, D. Daré-Emzivat, EMD-based filtering using similarity measure between probability density functions of IMFs, IEEE Transactions on Instrumentation and Measurement 63(1)(2014) 27-34.

[13] J.G. Teti. Jr., H.N. Kritikos, SAR ocean image representation Using wavelets, IEEE Transactions on Geoscience and Remote Sensing 30(5)(1992) 1089-1094.

[14] H.W. Liao, H.W. Huang, A multiple watermarking scheme for grey-level images using visual cryptography and integer wavelet transform, Journal of Computers 22(1)(2011) 18-36.

[15] H.L. Pu, S.W. Wen, H.W. Lu, L.A. Wu, X.J. Yang, Wavelet transform and its application in signal denoising, Modern Electronics Technique 35(19)(2012) 52-55.

[16] X.X. Chen, Y.J. Wang, L. Liu, Deep study on wavelet threshold method for image noise removing, Laser and Infrared 42(1)(2012) 105-110.

[17] L. Su, H.P. Nan, X.Y. Yu, L.C. Wu, J. Wang, Application of wavelet denoising of improved threshold function to vibration signal analysis of hydroelectric units, Journal of Hydroelectric Engineering 31(3)(2012) 246-251.

[18] L. Wang, Y.X. Shen, L.Y. Ji, Wind turbine gearbox fault diagnosis based on wavelet denoising and EMD, Journal of Jiangnan University 11(2)(2012) 159-162.

[19] B. Yan, J.H. Wang, J. Zhao, Research of image denoising technology based on mean filtering and wavelet transformation, Computer Technology and Development 21(2)(2011) 51-57.

[20] S. Gaci, The use of wavelet-based denoising techniques to enhance the first-arrival picking on seismic traces, IEEE Transactions on Geoscience and Remote Sensing 52(8)(2014) 4558-4563.

[21] A. Ahrabian, D.P. Mandic, A class of multivariate denoising algorithms based on synchrosqueezing, IEEE Transactions on Signal Processing 63(9)(2015) 2196-2208.

[22] W. Li, X.H. Chen, H.J. Mao, A study of adaptive optimal decomposition level in threshold denoising algorithm based on wavelet, Transform, Computer Simulation 26(3)(2009) 311-313.

[23] H.X. Yang, X.S. Wang, P.H. Xie, A.L. Leng, Y. Peng, Infrared image denoising based on improved threshold and inter-scale correlations of wavelet transform, ACTA Automatica Sinica 37(10)(2011) 1167-1174.

[24] Z. Wu, N.E. Huang, Ensemble empirical mode decomposition: a noise assisted method, Advances in Adaptive Data Analysis 1(1)(2009) 1-41.

[25] T. Qi, Y. Qiu, Y.F. Wu, Application of EEMD to suppression of mode mixing in oscillation signals, Noise and Vibration Control 30(2)(2010) 103-106.